Biochemistry and Biophysics Reports 38 (2024) 101722

Contents lists available at ScienceDirect

Biochemistry and Biophysics Reports

journal homepage: www.elsevier.com/locate/bbrep

Pan-cancer prognosis, immune infiltration, and drug resistance characterization of lung squamous cell carcinoma tumor microenvironment-related genes

Xiao Chen [a], Rui Li [b], Yun-Hong Yin [b], Xiao Liu [b], Xi-Jia Zhou [b], Yi-Qing Qu [b,*]

[a] Department of Respiratory Medicine, Tai'an City Central Hospital, Tai'an, China
[b] Department of Pulmonary and Critical Care Medicine, Qilu Hospital of Shandong University, Jinan, China

ARTICLE INFO

Keywords:
Tumor microenvironment
Pan-cancer analysis
Immune infiltrate
Drug resistance

ABSTRACT

Background: The tumor microenvironment (TME) plays an important role in cancer development; however, its implications in lung squamous cell carcinoma (LUSC) and pan-cancer have been poorly understood.
Methods: In this study, The Cancer Genome Atlas (TCGA) and Estimation of Stromal and Immune cells in Malignant Tumor tissue using Expression Data (ESTIMATE) datasets were applied to identify differentially expressed genes. Additionally, online public databases were utilized for in-depth bioinformatics analysis of pan-cancer datasets to investigate the prognostic implications of TME-related genes further.
Results: Our study demonstrated a significant association between stromal scores, immune scores, and specific clinical characteristics in LUSC patients. C3AR1, CSF1R, CCL2, CCR1, and CD14 were identified as prognostic genes related to the TME. All TME-related prognostic genes demonstrated varying degrees of correlation with immune infiltration subtypes and tumor cell stemness. Moreover, our study revealed that TME-related prognostic genes, particularly C3AR1 and CCR1, might contribute to drug resistance in cancer cells.
Conclusions: The identified TME-related prognostic genes, particularly C3AR1 and CCR1, have potential implications for understanding and targeting drug resistance mechanisms in cancer cells.

1. Introduction

Recent statistical data, indicate that lung cancer continues to be the most lethal type of malignancy globally, resulting in an estimated 1.76 million deaths and affecting 2.09 million individuals annually [1,2]. Histological analyses have demonstrated that the majority of lung cancer cases (approximately 85 %) are classified as non-small cell lung cancer (NSCLC) [3,4]. The implementation of targeted therapies for mutated genes, including EGFR, ALK, ROS1, HER2, AKT1, RET, and BRAF, has improved clinical outcomes in patients with lung adenocarcinoma (LUAD) [5,6]. However, despite being the second most prevalent subtype of NSCLC with rising mortality rates, targeted genes accessible for LUSC patients are limited [7]. Consequently, the identification of new biomarkers for LUSC is imperative for developing targeted therapies. Cancer immunotherapy, recognized as one of the most promising approaches for cancer treatment, is gaining attention [8]. Epigenetic regulation within the TME significantly influences tumor progression, invasion, metastasis, and drug resistance [8]. Additionally, studies have shown that immune tolerance and evasion in the TME of LUSC can be facilitated by various mechanisms. Consequently, understanding the complexities of the LUSC microenvironment is crucial.

The TME plays a critical role in tumor initiation, advancement, and metastasis [9]. Therefore, this is an appealing target for developing novel cancer treatment approaches. Both immune and stromal cells are recognized for their significant contributions to tumor communication, immune monitoring, and the formation of tumor niches [10]. Immune score has been utilized as a prognostic indicator in the diagnosis and prognosis of various cancers [11]. Research suggests that stromal cells within the TME play a role in maintaining genetic stability, making them promising therapeutic targets with reduced risks of drug resistance and tumor recurrence [12]. Immunotherapeutic approaches, including immune checkpoint inhibitors and CAR-T cell therapy, offer promising prospects in cancer treatment [13]. Additionally, studies have demonstrated the potential of utilizing modified TCR-T cells in preclinical and clinical research [13]. The dysregulated metabolic activity in tumor cells can induce metabolic stress in tumor-infiltrating immune cells,

* Corresponding author. Department of Pulmonary and Critical Care Medicine, Qilu Hospital of Shandong University, Wenhuaxi Road 107#, Jinan, China.
E-mail address: quyiqing@sdu.edu.cn (Y.-Q. Qu).

https://doi.org/10.1016/j.bbrep.2024.101722
Received 16 November 2023; Received in revised form 21 April 2024; Accepted 24 April 2024

compromising their antitumor immune responses [14]. Mutations in cancer therapeutic targets can significantly affect drug sensitivity, leading to the emergence of drug resistance [14]. Consequently, developing multi-target strategies to inhibit TME components may provide a more effective approach to cancer treatment.

The Estimation of STromal and Immune cells in MAlignant Tumors using Expression data (ESTIMATE) algorithm offers an effective method for estimating the diagnostic and prognostic significance of immune and stromal cells in various malignancies, including renal cell carcinoma (RCC), thyroid cancer, and glioblastoma [15]. Xiao et al. [12] identified three prognostic markers, CASKIN1, EMR3, and GBP5, associated with TME in hepatocellular carcinoma (HCC), indicating their potential as targeted immunotherapy candidates in liver cancer. A recent study used the algorithm to predict the prognosis and characterize the immune microenvironment of LUAD [16]. Nevertheless, the specific contribution of immune and stromal cells within the TME of LUSC remains ambiguous and necessitates further exploration using the ESTIMATE algorithm.

In this study, RNA expression patterns and clinical characteristics of individuals diagnosed with LUSC were obtained from The Cancer Genome Atlas (TCGA) database [17]. The main aim of this research was to examine the correlation between clinical characteristics and the ESTIMATE score, as well as to investigate the impact of TME-related genes on the prognosis of patients with LUSC. Additionally, a range of databases, such as ONCOMINE, the Human Protein Atlas (HPA), cBioPortal, and TIMER 2.0, were employed to assess the prognostic relevance of genes in LUSC patients. It is worth noting that TCGA pan-cancer data were utilized to evaluate the expression of TME-related genes across 33 different types of cancer and their association with overall survival (OS). Furthermore, a relationship was identified between the expression of these genes within TME and their corresponding pharmacological effects.

2. Materials and methods

2.1. Microarray data

This study aimed to evaluate the gene expression profiles of patients diagnosed with LUSC. Transcriptomic data from the TCGA database were acquired and analyzed for differential gene expression using FPKM values. Following the successful download and conversion of the data, the ESTIMATE algorithm was utilized to calculate the stromal and immune scores [18].

2.2. Identification of differentially expressed genes (DEGs)

Differential gene expression analysis was performed using the "limma R″ package [19]. DEGs were identified based on a cutoff fold change value of (log FC) > 1 and an adjusted false discovery rate (FDR) of $p < 0.05$. Subsequently, patients were divided into low and high immune/stromal score groups according to these criteria. Comparative analyses of immune/stromal scores were then conducted for various clinical features. Heatmaps were generated for stromal and immune cells utilizing the "pheatmap R package, followed by clustering analysis. $P < 0.05$ was considered a statistically significant difference.

2.3. Enrichment analysis of DEGs

DEGs were filtered using the R software with the Venn diagram package, and a subset of overlapping DEGs was selected for further analysis. The functional significance of these DEGs was determined using Gene Ontology (GO) analysis and Kyoto Encyclopedia of Genes and Genomes (KEGG) pathway analyses, with statistical significance set at $p < 0.05$.

2.4. Identification of TME-related prognostic genes

The prognostic potential of DEGs in LUSC was evaluated in groups with low and high stromal/immune scores utilizing the R software. $P < 0.05$ was considered statistically significant, indicating the identification of relevant target genes. Subsequent analyses included the creation of a protein–protein interaction (PPI) network using STRING [20] and the construction of a bar plot using R software. The top-ranked DEGs were selected as crucial TME-related prognostic genes.

2.5. Overall survival analysis

The prognostic significance of TME-associated genes was evaluated in this study using Gene Expression Profiling Interactive Analysis (GEPIA), a recently introduced interactive web-based tool for analyzing normal and neoplastic gene expression patterns [21]. A statistical significance threshold of $p < 0.05$ was applied.

2.6. The Human Protein Atlas

Immunohistochemistry (IHC) analysis was performed to assess the protein expression levels of TME-associated prognostic genes in LUSC samples. The Human Protein Atlas (HPA), comprising of six different sections with publicly available data, includes the tissue atlas, which represents the protein distribution in the major organs and tissues of the human body [22].

2.7. Comprehensive analysis of TME-related prognostic genes in LUSC

Tumor Immune Estimation Resource (TIMER), a computational resource for analyzing tumor-infiltrating immune cells, was used to investigate the associations between hub genes and these cells [23]. The mutation and gene-outcome module of TIMER was employed to evaluate the clinical relevance and influence of gene mutations on immune cell infiltration. To investigate the TME-related prognostic genes, the LUSC (TCGA, PanCancer Atlas) dataset was analyzed using cBioPortal [24]. The OncoPrint feature was utilized to graphically represent genetic alterations in the hub genes in each sample. Moreover, the co-expression of TME-related prognostic genes was calculated using the cBioPortal online tool. Subsequently, variations in transcription levels between samples were assessed using the *t*-test in the ONCOMINE database [25]. TIMER Gene-DE functionality revealed the differential expression of TME-related prognostic genes in normal and tumor tissues ($^{*}p < 0.05$; $^{**}p < 0.01$; $^{***}p < 0.001$).

2.8. TCGA pan-cancer data acquisition and analysis

The transcription data, clinical data, stemness scores based on DNA methylation (DNAss) and mRNA (RNAss), phenotype-immune subtype data, and other relevant information were obtained from the UCSC Xena browser (https://xenabrowser.net). The TCGA pan-cancer dataset included 33 cancer types: ACC, BLCA, BRCA, CESC, CHOL, COAD, DLBC, ESCA, GBM, HNSC, KICH, KIRC, KIRP, LAML, LGG, LIHC, LUAD, LUSC, MESO, OV, PAAD, PCPG, PRAD, READ, SARC, SKCM, STAD, TGCT, THCA, THYM, UCEC, UCS, and UVM. Notably, 15 cancer types had fewer than five normal tissue samples or none at all. Accordingly, we used a linear mixed-effects model to statistically compare the TME-related prognostic gene expression in the normal and tumor tissues of 18 cancer types [26]. Subsequently, the differential expression levels of TME-related prognostic genes in 18 tumors were assessed using the "corrplot" R package to determine their potential significance. The association between the expression of these genes and OS was further analyzed using survival analysis of all tumor samples, with statistical significance set at $p < 0.05$.

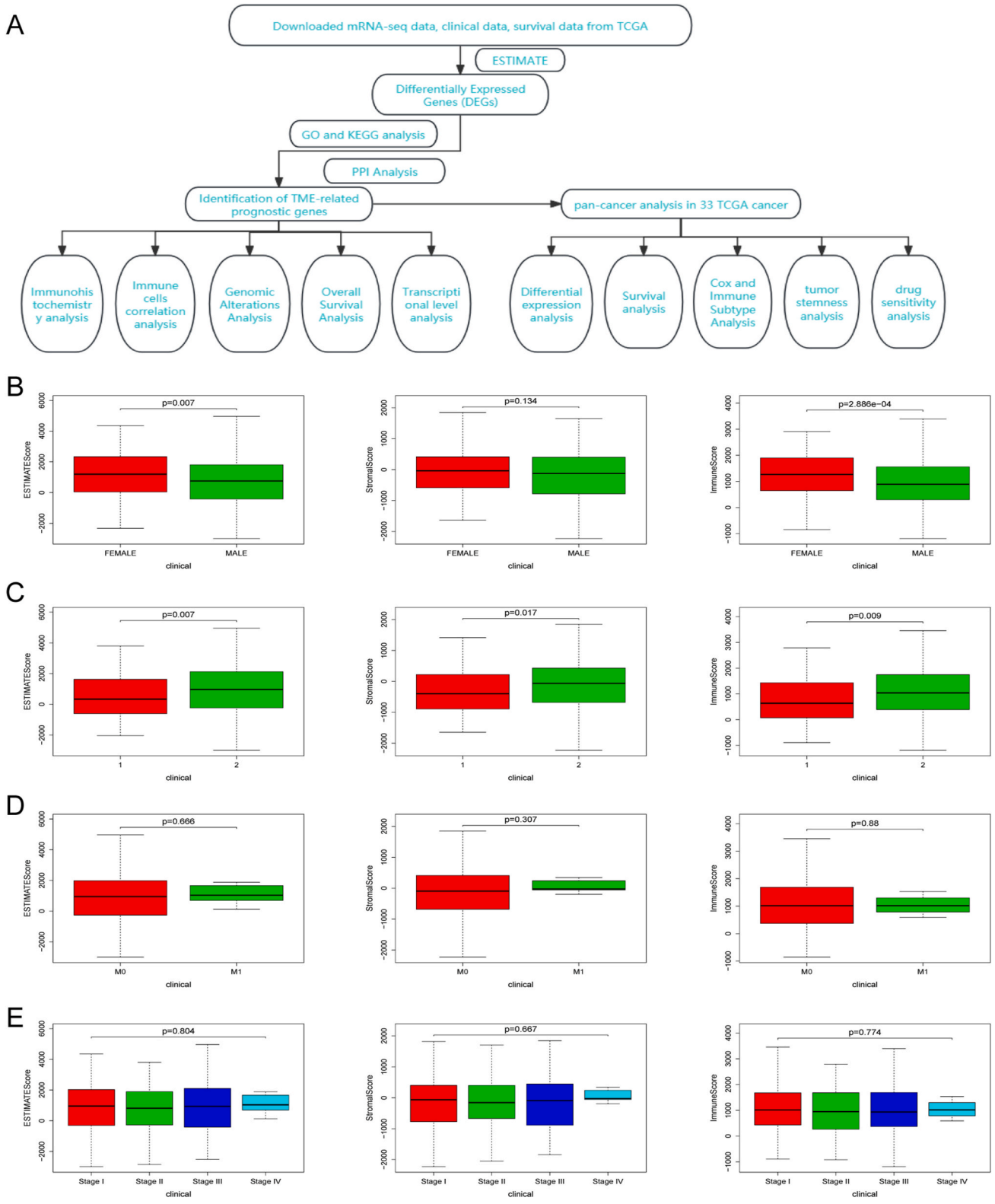

Fig. 1. Flowchart of the manuscript and associations between immune/stromal scores and clinical characteristics of LUSC patients. (**A**) Flowchart of the manuscript. (**B**) A significant association was observed between gender and the immune score ($p = 2.886e\text{-}04$) or the ESTIMATE score ($p = 0.007$). (**C**) A significant association was observed between age ($1 < 60$, and $2 \geq 60$) and the immune score ($p = 0.009$), stromal score ($p = 0.017$), and ESTIMATE score ($p = 0.007$). (**D**) LUSC patients with distant metastases exhibited higher immune scores ($p = 0.88$, median scores 1034.73 vs. 1016.71), stromal scores ($p = 0.307$, median scores 56.57 vs. −95.23), and ESTIMATE scores ($p = 0.666$, median scores 1253.27 vs. 948.14); these differences were not statistically significant. (**E**) Patients with stage IV disease exhibited higher stromal scores (median scores of −25.95 vs. −65.06) and ESTIMATE scores (median scores of 1038.32 vs. 956.59) than patients with stage I disease, with no statistically significant differences.

Table 1
The baseline characteristics of all patients.

Variables	Subtype	Count	Percent (%)
Age(years)	<60	87	17.98
	≥60	397	82.02
Gender	Female	126	26.03
	Male	358	73.97
Stage	I	238	49.17
	II	157	32.44
	III	82	16.94
	IV	7	1.45
T (Tumor)	T1	110	22.73
	T2	284	58.68
	T3	68	14.05
	T4	22	4.54
N (Node)	N0	308	63.64
	N1	127	26.24
	N2	38	7.85
	N3	5	1.03
	Nx	6	1.24
M (Metastasis)	M0	401	82.85
	M1	7	1.45
	Mx	76	15.70
Total		484	100

2.9. Analysis of immune subtypes, tumor stemness features and drug sensitivity of TME-related prognostic genes

Six distinct immune subtypes were evaluated to identify immune infiltration within the TME [27]. The relationship between TME-related prognostic gene expression and immune infiltration type was evaluated using ANOVA models. Additionally, the stem cell-like properties of tumor cells were evaluated by calculating the tumor stemness scores based on transcriptome and epigenetic data from TCGA cancer samples. The Spearman's correlation test was then employed to assess the association between tumor stemness and the expression of TME-related prognostic genes. $P < 0.05$ was considered a statistically significant difference.

3. Results

3.1. Patient characteristics

Gene expression data and comprehensive clinical characteristics of 484 patients with LUSC were obtained from the TCGA database. A flow diagram illustrating the manuscript is depicted in Fig. 1A, and the patients' demographic and baseline characteristics are listed in Table 1.

3.2. Evaluation of stromal and immune scores

The complete gene expression profiles and clinicopathological data of all 484 patients with LUSC were obtained from the TCGA database. Analysis revealed that immune scores ($p = 2.886e-04$) and ESTIMATE scores ($p = 0.007$) were significantly higher in female LUSC patients compared to their male counterparts (Fig. 1B). Moreover, advanced age was associated with higher ESTIMATE scores ($p = 0.007$), immune scores ($p = 0.009$), and stromal scores ($p = 0.017$) (Fig. 1C). Although statistically insignificant, LUSC patients with distant metastases had higher immune scores (Fig. 1D, $p = 0.88$; median scores 1034.73 vs. 1016.71), stromal scores ($p = 0.307$; median scores 56.57 vs. −95.23), and ESTIMATE scores ($p = 0.666$; median scores 1253.27 vs. 948.14). Additionally, stage IV patients demonstrated higher stromal scores (median scores −25.95 vs. −65.06) and ESTIMATE scores (median scores 1038.32 vs. 956.59) compared to stage I patients; however, the differences were not statistically significant (Fig. 1E).

The LUSC patient cohort was categorized into high- and low-score groups based on their respective scores. Analysis of the ESTIMATE score revealed a longer OS in LUSC patients in the low-score group compared to those in the high-score group (Fig. 2A, median 539 days vs. 587 days, $p = 0.05$). Similarly, the stromal (Fig. 2B, median 513.5 days vs. 585 days, $p = 0.066$) and immune (Fig. 2C, median 535 days vs. 581 days, $p = 0.219$) score results demonstrated a longer median OS in the low-score group of LUSC patients than the high-score group, without statistically significant difference.

3.3. Comparison of gene expression profiles with stromal scores and immune scores in LUSC

The heatmaps illustrating gene expression patterns based on stromal score (Fig. 2D), revealed that 1195 genes were upregulated and 136 genes were downregulated in the high-score group compared to those in the low-score group ($p < 0.05$). Similarly, the heatmaps based on the immune score (Fig. 2E), revealed 1187 upregulated and 176 downregulated genes in the high-score group compared to the low-score group ($p < 0.05$). Additionally, Venn diagrams revealed that 874 genes were upregulated (Fig. 2F), whereas 72 genes were downregulated (Fig. 2G).

3.4. Functional enrichment analysis of DEGs

The results of the GO analysis for the top 10 biological processes (BP), cellular components (CC), and molecular functions (MF) are presented in Fig. 3A. The six enriched BPs included T-cell activation, leukocyte migration, leukocyte proliferation, leukocyte cell–cell adhesion, lymphocyte proliferation, and mononuclear cell proliferation. These BPs are integral to immune cells differentiation and activation. The top six CCs identified in this study included the external side of the plasma membrane, secretory granule membrane, collagen-containing extracellular matrix, MHC class II protein complex, tertiary granule, and tertiary granule membrane. These CCs were involved in extracellular matrix and membrane functions. The top six enriched MFs included carbohydrate binding, cytokine receptor activity, cytokine binding, immunoglobulin binding, glycosaminoglycan binding, chemokine activity, and chemokine receptor binding. These MFs are primarily related to surface receptor activity and protein binding. KEGG analysis (Fig. 3B) indicated that DEG-related pathways were significantly associated with the immune response.

3.5. PPI network and identification of TME-related hub genes

In this study, 154 target genes were selected. The log-rank test indicated a statistically significant association with poor OS prediction in LUSC ($p < 0.05$). The PPI network was constructed utilizing the online STRING tool, yielding a functional network comprising 153 nodes and 281 edges (Fig. 3C). Analysis of the PPI network, indicated that the top six significant genes (C3AR1, CSF1R, CCL2, CCR1, TYROBP, and CD14) were TME-related hub genes (Fig. 3D).

3.6. The roles of TME-related hub genes in OS in LUSC patients

The log-rank test was conducted for six TME-related hub genes, specifically C3AR1, CSF1R, CCL2, CCR1, TYROBP, and CD14, indicating a significant association with OS in patients with LUSC, with the exception of TYROBP (Fig. 4A-F, $p < 0.05$). Furthermore, the expression levels of all six genes differed significantly (Fig. 4G-L, $p < 0.05$). Therefore, the following five TME-related hub genes were selected for further analysis: C3AR1, CSF1R, CCL2, CCR1, and CD14.

3.7. Immunohistochemistry of the five TME-related hub genes

IHC analysis of the five hub genes related to the TME was performed using data obtained from the HPA. The findings indicated a significant decrease in the protein expression levels of C3AR1, CCL2, and CD14 in tumor tissues compared to normal tissues, while the protein expression

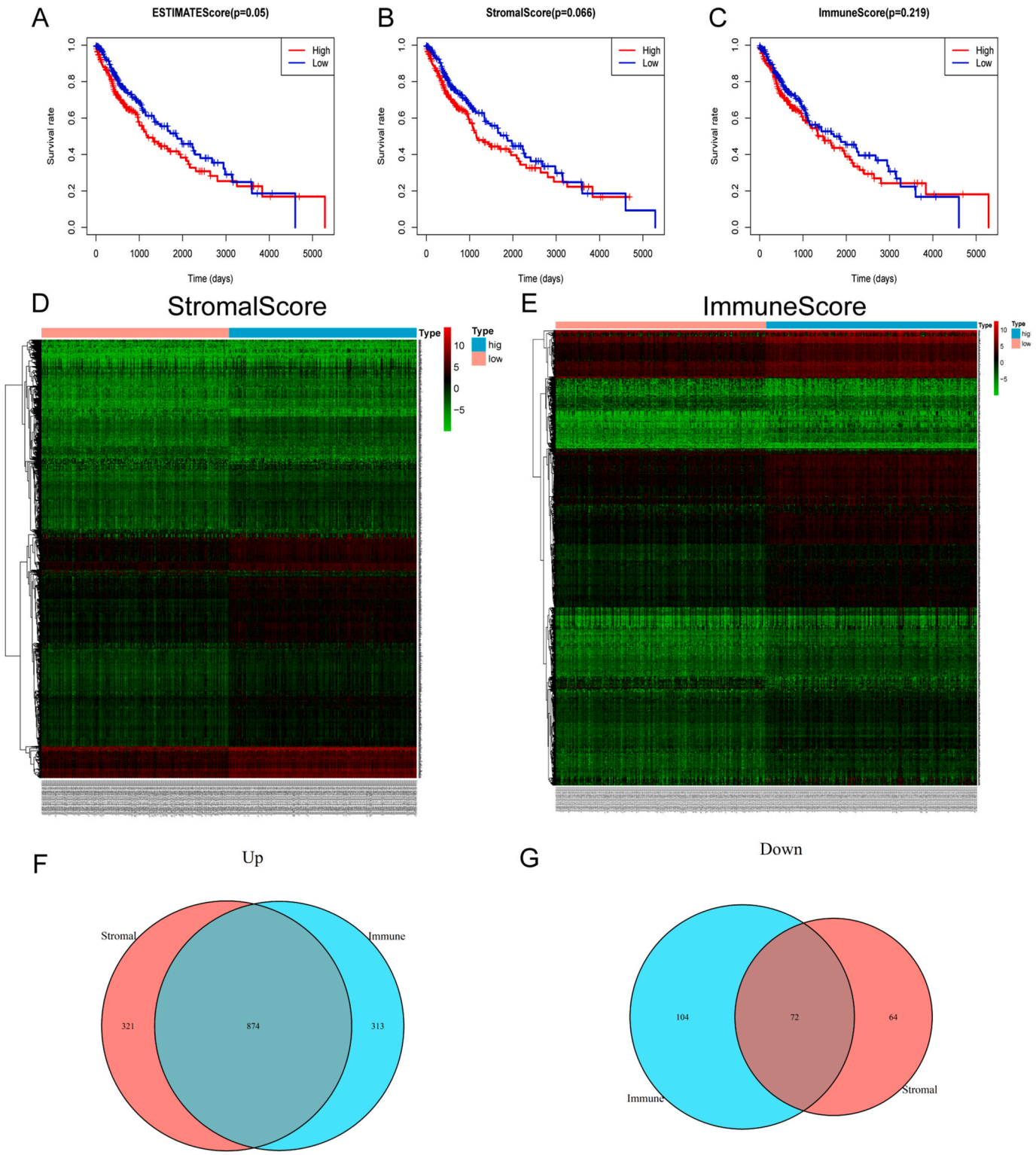

Fig. 2. OS and comparison of gene expression profiles with immune and stromal scores in LUSC. (**A**) OS in LUSC patients with high ESTIMATE scores was lower than in patients with low ESTIMATE scores ($p = 0.05$). (**B**) OS in LUSC patients with high stromal scores was lower than in patients with low stromal immune scores ($p = 0.066$). (**C**) OS in LUSC patients with high immune scores was lower than in patients with low immune scores ($p = 0.219$). (**D**) Heatmap of DEGs in the stromal score comparison between the high- and low-score groups (fold change>1, $p < 0.05$). (**E**) Heatmap of DEGs in the immune score comparison between the high- and low-score groups (fold change>1, $p < 0.05$). The number of upregulated (**F**) or downregulated (**G**) DEGs in the immune and stromal score groups.

level of CSF1R was significantly higher in tumor tissues. However, we were unable to conclusively determine the protein levels of CCR1. The protein levels of C3AR1 in normal and tumor tissue samples were depicted in Fig. 5A, while Fig. 5B illustrated the protein levels of CSF1R in comparable samples. Similarly, the protein levels of CCL2 and CD14, in the normal and tumor tissues are shown in Fig. 5C-D, respectively.

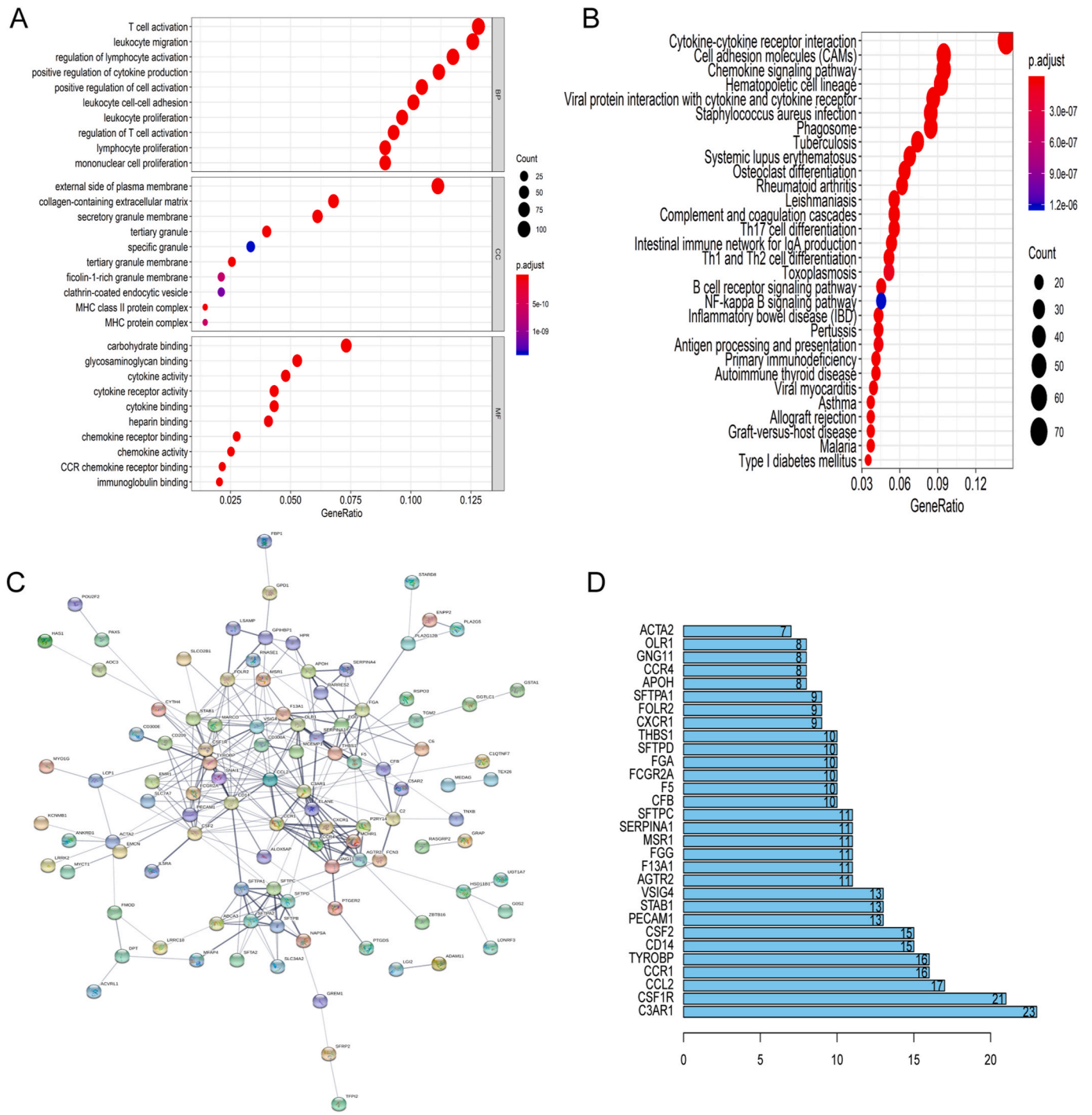

Fig. 3. Functional enrichment analyses of DEGs and identification of TME-related hub genes. (**A**) The top 10 terms in the GO (BP, CC, MF) analysis with $p < 0.05$. (**B**) $P < 0.05$ for the top 30 terms in the KEGG pathway analysis. (**C**) PPI networks were drawn using the STRING tool at a median confidence interval of 0.400 (153 nodes and 281 edges). (**D**) Bar plotof the significant genes in the PPI network.

3.8. The correlation between TME-related hub genes and immune cell infiltration

A positive correlation was observed between the expression levels of TME-related hub genes, C3AR1, CSF1R, CCL2, CCR1, and CD14, and immune cell infiltration (Fig. 6A–E). Additional information was detailed in Table 2. Kaplan–Meier survival curves were generated for the hub genes utilizing gene-outcome analysis, revealing that patients with high expression levels of all five genes experienced a significantly worse prognosis ($p < 0.05$) (Fig. 6F).

3.9. Genomic alterations and co-expression of TME-related hub genes in LUSC

The cBioPortal online tool 'OncoPrint' was used to detect the genomic alterations (Fig. 7A). The results revealed that TME-related hub genes were altered in 74 of 487 patients (15 %). The mutation rates of C3AR1, CSF1R, CCL2, CCR1, and CD14 were 8 %, 5 %, 3 %, 2.7 %, and 2.1 %, respectively. Moreover, a co-expression analysis was conducted to ascertain the correlation between various TME-related hub genes. A statistically significant positive interaction was observed among all pairs

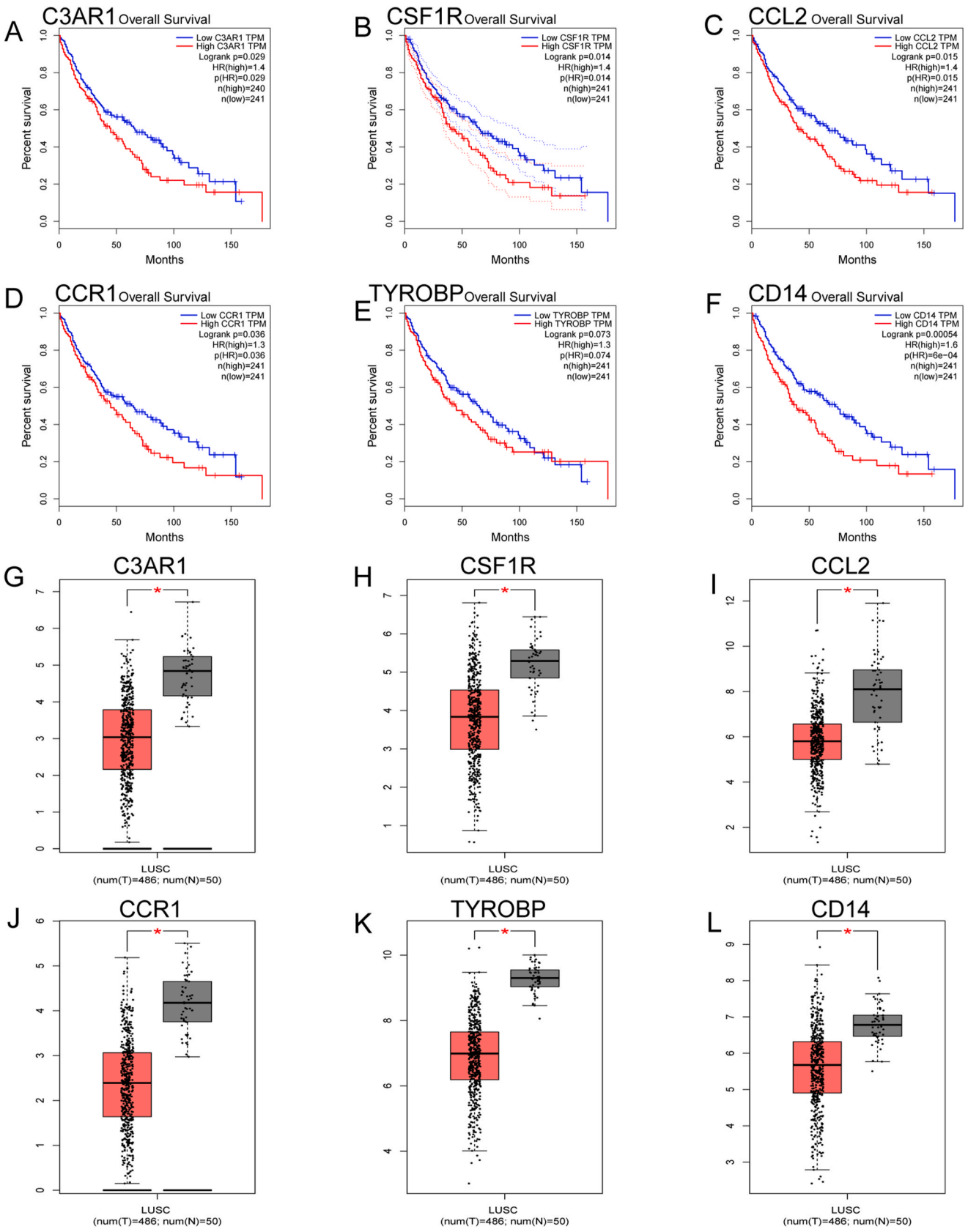

Fig. 4. Correlation between the expression of TME-related hub genes and OS in LUSC patients. **(A-F)** Kaplan–Meier survival curves were generated for hub genes (C3AR1, CSF1R, CCL2, CCR1, TYROBP, and CD14) obtained from the comparison of groups with high (red line) and low (blue line) gene expression. **(G–L)** Box plots of the tumor (red) and normal (gray) expression.

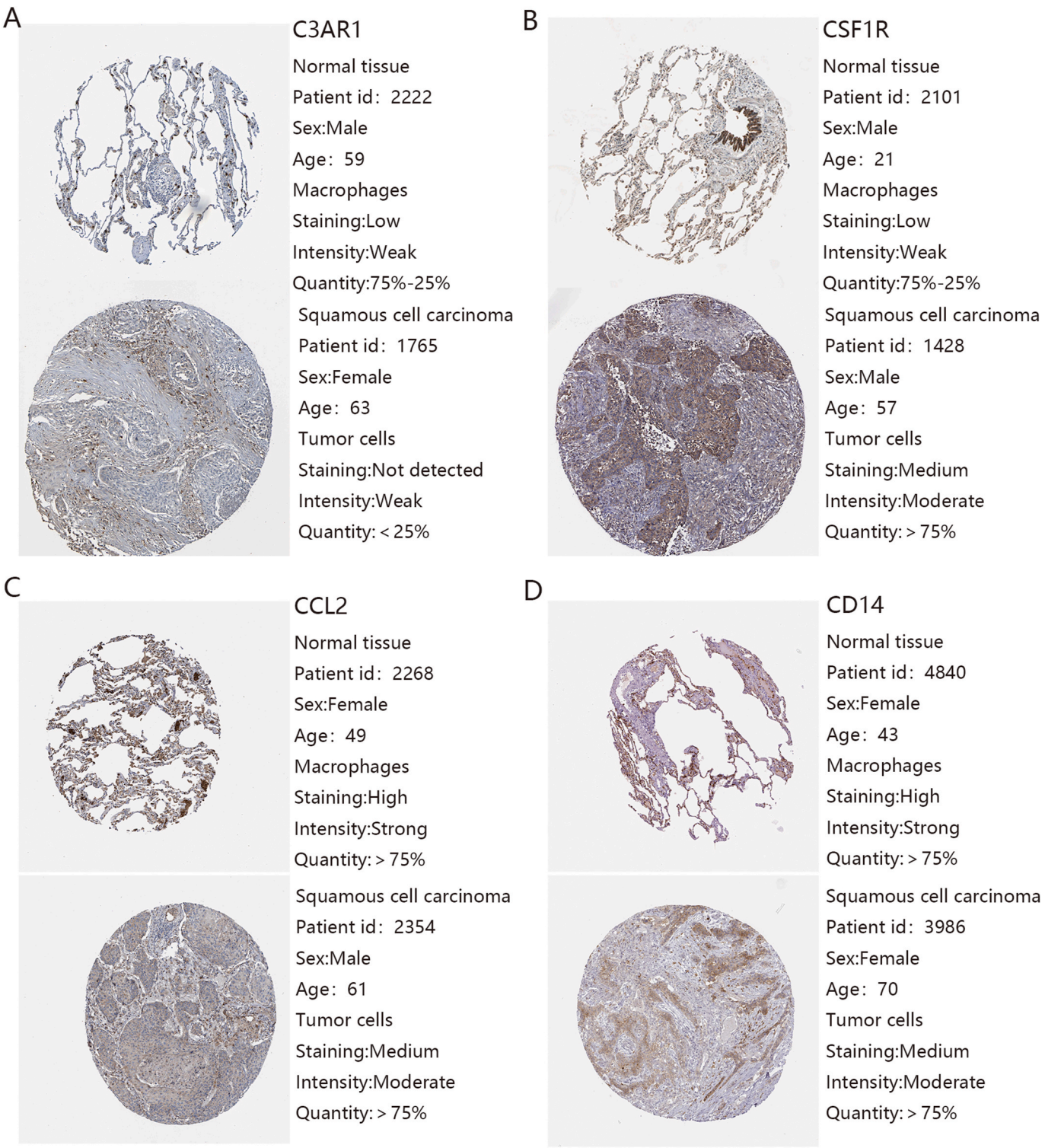

Fig. 5. Immunohistochemistry of the five TME-related hub genes. (**A**) Protein levels of C3AR1 in normal tissue and tumor tissue. (**B**) Protein levels of CSF1R in normal tissue and tumor tissue. (**C**) Protein levels of CCL2 in normal tissue and tumor tissue. (**D**) Protein levels of CD14 in normal tissue and tumor tissue.

of hub genes (Fig. 7B and Table 3). Furthermore, the impact of gene mutations on immune infiltration was determined using TIMER, with a significance threshold of $p < 0.05$ (Table 4). Our findings revealed increased immune cell infiltration, specifically macrophages (C3AR1 and CSF1R) and $CD4^+$ T cells (CSF1R), in relation to gene mutations (Fig. 7C).

3.10. Expression and mRNA expression of TME-related hub genes in LUSC patients

The TIMER analysis of 501 tumor patients and 51 normal patients revealed significant differential expression of TME-related hub genes (Fig. 7D, $p < 0.001$). The transcriptional levels of TME-related hub genes in cancerous and normal tissues were compared using ONCOMINE analysis (Fig. 7E). The expressions of C3AR1, CCL2, and CCR1 in LUSC

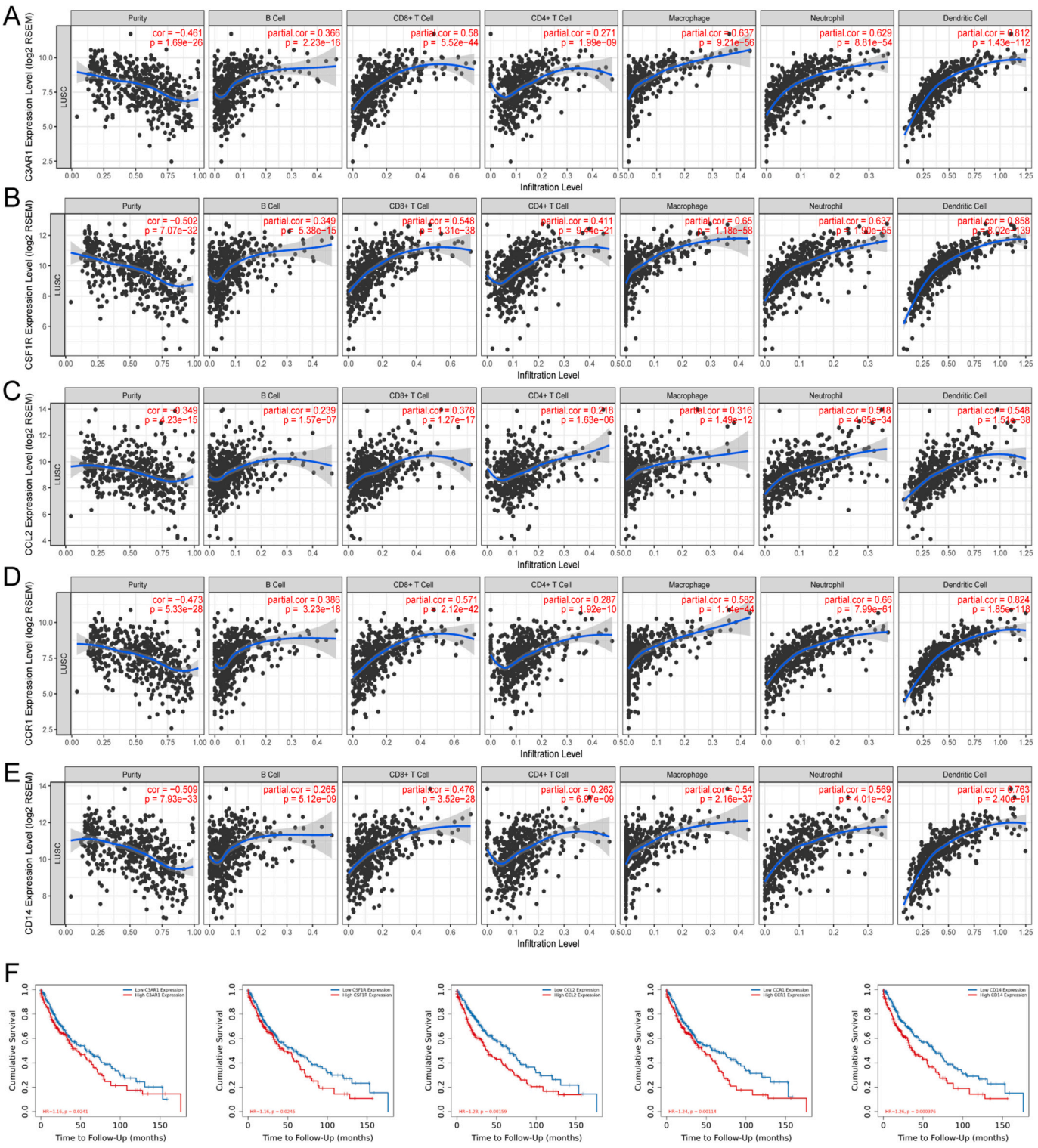

Fig. 6. The correlation between TME-related hub genes and immune cell infiltration and the KM curve of TME-related hub genes. There were positive correlations between TME-related hub gene expression and immune cell infiltration (C3AR1 Fig.6A, CSF1R Fig.6B, CCL2 Fig.6C, CCR1 Fig.6D, and CD14 Fig.6E). The KM curve of the TME-related hub genes (Fig.6F, $p < 0.05$).

tissues were lower than that in normal tissues (Table 5); however, CD14 expression was undetected in LUSC.

3.11. *Expression of TME-related prognostic genes in pan-cancers*

To determine the internal expression patterns of the five TME-related prognostic genes, their expression levels were analyzed across all 33 cancer types in the TCGA pan-cancer dataset. The results indicated significant heterogeneity in both intra- and inter-tumor expression of these genes (Fig. 8A). Particularly, CCR1 exhibited comparatively lower average expression levels across all cancer types than CD14 (Fig. 8A).

The expression levels of all five genes across 18 different cancer types were analyzed in this study, each within a minimum of 5 paired adjacent normal samples. Our findings revealed significant variations in the

Table 2
The correlation between TME-related hub genes and immune cell infiltration.

variable		C3AR1	CCL2	CCR1	CD14	CSF1R	PECAM1	STAB1	TYROBP	VSIG4
B Cell	cor	0.366	0.239	0.386	0.265	0.349	0.443	0.162	0.375	0.297
	p	2.23E-16	1.57E-07	3.23E-18	5.12E-09	5.38E-15	4.64E-24	0.000410954	3.65E-17	4.64E-11
$CD8^+$ T Cell	cor	0.560	0.378	0.571	0.476	0.548	0.475	0.331	0.522	0.486
	p	5.52E-44	1.27E-17	2.12E-42	3.52E-28	1.31E-38	3.78E-28	1.27E-13	1.39E-34	1.65E-29
$CD4^+$ T Cell	cor	0.271	0.218	0.287	0.262	0.411	0.349	0.492	0.221	0.165
	p	1.99E-09	1.63E-06	1.92E-10	6.97E-09	9.44E-21	4.33E-15	2.94E-30	1.15E-06	0.000312443
Macrophage	cor	0.637	0.316	0.582	0.540	0.650	0.524	0.535	0.531	0.616
	p	9.21E-56	1.49E-12	1.14E-44	2.16E-37	1.18E-58	5.35E-35	1.25E-36	4.90E-36	3.65E-51
Neutrophil	cor	0.629	0.518	0.660	0.569	0.637	0.472	0.545	0.513	0.517
	p	8.81E-54	4.65E-34	7.99E-61	4.01E-42	1.90E-55	9.60E-28	3.33E-38	2.34E-33	6.69E-34
Dendritic Cell	cor	0.812	0.548	0.824	0.763	0.858	0.610	0.625	0.740	0.687
	p	1.43E-112	1.51E-38	1.85E-118	2.40E-91	8.02E-139	1.50E-49	1.14E-52	1.83E-83	1.51E-67

expression of TME-related prognostic genes among the different tumor types (Fig. 8B). CCR1 and C3AR1 were predominantly upregulated in the tumors studied, while CCL2 was predominantly downregulation, with only a few exceptions. The expression levels of C3AR1, CSF1R, CCL2, CCR1, and CD14 in 18 individual tumor tissues are depicted in Fig. 8C-G. Variations in expression were observed in four tumors: COAD, LUAD, LUSC, and THCA. Within this subset of genes, COAD, LUAD, and LUSC exhibited low expression levels across all five genes, while THCA revealed low expression only in CCL2, with the remaining genes exhibiting high expression levels. Besides, Spearman's correlation analysis revealed positive correlations between the expression levels of various TME-related genes. The strong correlation between CSF1R and C3AR1 indicates potential shared characteristics or functions ($r = 0.90$, $p < 0.001$) (Fig. 8H).

3.12. Association of TME-related gene expression with OS

An analysis involving 33 cancer types was conducted to investigate the association between TME-related gene expression and OS, with the aim of identifying prognostic genes that may promote or inhibit tumorigenesis in specific tumor types. The univariate Cox proportional hazards regression model revealed a statistically significant association ($p < 0.05$). The results of our study indicate that alterations in predicted TME-related predicted gene expression were consistently associated with differences in patient survival outcomes. However, the specific nature of these relationships varied significantly depending on the individual gene and the type of cancer (Fig. 9).

This study revealed that C3AR1 was indicative of unfavorable prognostic outcomes in patients with UVM, TGCT, and LGG, while exhibiting a correlation with improved survival rates in patients with SKCM and KIRP (Fig. 10A). Additionally, CSF1R was associated with poor prognosis in THYM patients but was associated with better survival in patients with ACC and SKCM (Fig. 10B). Similarly, CCL2 was identified a predictor of poor prognosis in THYM, LUSC, and GBM patients, with the exception of SKCM patients, exhibiting poor survival outcome only in (Fig. 10C). Moreover, elevated expression levels of CCR1 were indicative of poor prognosis in UVM and LGG patients, while conferring a survival advantage for OV, SKCM, and MESO patients (Fig. 10D). CD14 was associated with unfavorable outcomes in patients with THYM, TGCT, KIRC, and LUSC, while positively affecting the survival of patients with SKCM and ACC (Fig. 10E). A significant correlation was observed between all TME-related prognostic genes and OS across all examined cancer types, especially in SKCM patients, where elevated expression levels were indicative of a favorable prognosis ($p < 0.001$).

3.13. Association of TME-related prognostic gene expression with immune response and tumor stemness

The primary objective of this study was to determine the relationship between TME-related gene expression and immune cell infiltration patterns in various types of cancer. In this study, six types of immune infiltration in human tumors were classified, ranging from tumor promoting to tumor inhibiting, including C1 (wound healing), C2 (INF-γ dominated), C3 (inflammatory), C4 (lymphocyte depleted), C5 (immunologically quiet), and C6 (TGF-β dominant) [28]. Analysis of TCGA pan-cancer data revealed a significant association between the elevated expression levels of TME-related genes and C6. This correlation suggested that the identified genes were significantly involved in promoting tumor growth, as evidenced by the lower survival rates and higher TGF-β enrichment observed in patients within these categories (Fig. 11A).

Moreover, tumor stemness was evaluated using RNA stemness scores based on mRNA expression (RNAss) and DNA stemness scores based on DNA methylation patterns (DNAss) [29]. The results indicated that TME-related genes exhibited varying correlations with RNAss and DNAss in different cancers (Fig. 11B-C). However, a negative correlation was observed between TME-related genes and RNAss, except for KIRC and MESD ($p < 0.0001$), where CSF1R exhibited strongest correlation ($r = -0.78$). Additionally, TME-related genes were positively correlated with DNAss ($p < 0.0001$) in ACC, OV, THCA, THYM, and UVM.

3.14. TME-related genes were associated with the sensitivity of cancer cells to chemotherapy

The expression of TME-related genes in the NCI-60 cell line and their association with drug sensitivity were evaluated using a wide array of over 200 chemotherapeutic drugs. The results indicated significant diversity in the expression of TME-related genes among the different cell lines (Fig. 12). A positive association was observed between elevated expression of TME-related genes, particularly CCR1 and C3AR1, and increased resistance to multiple chemotherapeutic agents ($r > 0.4$, $p < 0.0001$) across various cell lines. CCR1 and C3AR1 were associated with drug resistance to several chemotherapeutics, including Denileukin Diftitox (Ontak), alectinib, isotretinoin, estramustine, and carmustine. Additionally, our results revealed that specific TME-related genes influence the sensitivity to multiple drugs.

4. Discussion

Lung cancer is a fatal disease globally, with NSCLC being the primary cause of cancer-related deaths [30]. In the immune microenvironment, prognosis and prediction markers have significantly improved lung cancer treatment outcomes, particularly in patients with adenocarcinoma [31].The TME is an intricate network of tissues that plays a crucial role in regulating the immune response against tumors through immune and stromal cell interactions. Recent research has shown that markers present in the TME can serve as prognostic indicators for tumors. Zeng et al. conducted a thorough analysis of the TME characteristics in gastric cancer and proposed innovative treatment strategies [32]. Similarly, another study highlighted the prognostic value of an immune-inflamed TME in LUAD [33]. Moreover, Yue et al. identified three DEGs related to TME that could predict the prognosis of patients with LUAD [34]. Currently, targeted therapy for LUSC remains a challenge. In contrast to

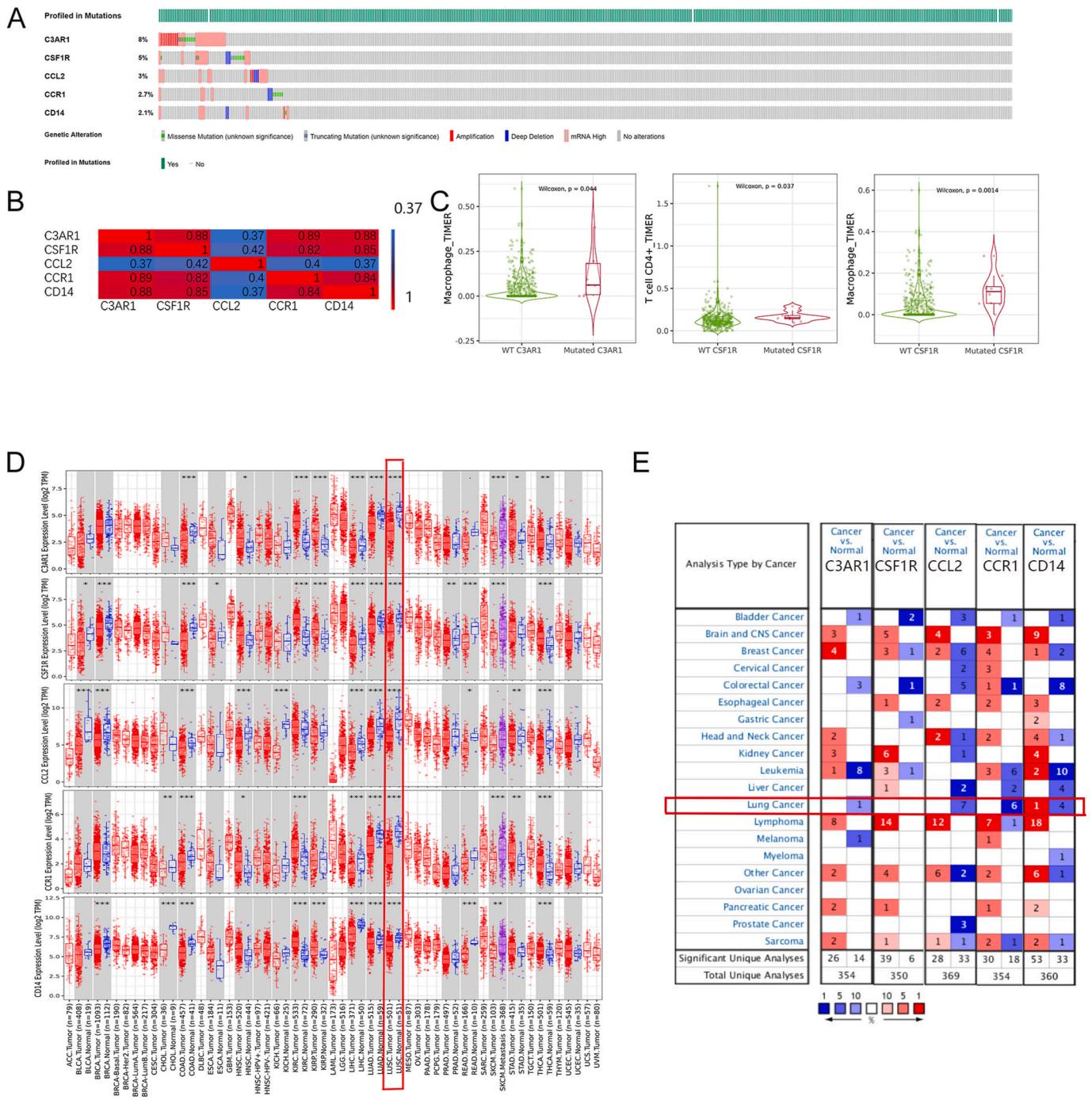

Fig. 7. Genomic alterations and expression of TME-related hub genes in LUSC. (**A**) Genomic alterations in the hub genes. The mutation rates of C3AR1, CSF1R, CCL2, CCR1 and CD14 were 8 %, 5 %, 3 %, 2.7 %, and 2.1 %, respectively. (**B**) Correlation between any two TME-related hub genes. (**C**) Violin plots of the effect of TME-related gene mutations on immune cell infiltration according to TIMER ($p < 0.05$). (**D**) Differential expression of TME-related hub genes according to TIMER ($p < 0.001$). (**E**) Transcriptional levels of TME-related hub genes in normal tissues were determined by ONCOMINE.

LUAD, LUSC exhibited with intricate molecular features, including a scarcity of prevalent driver gene mutations and therapeutic targets. However, progress in biotechnological advancements and pharmaceutical research has propelled the investigation and development of prospective targeted therapeutic interventions. The amalgamation of individualized treatment modalities, exploration of novel drug targets, and implementation of a comprehensive treatment regimen could augment the efficacy of therapeutic interventions and improve the OS rates of patients with LUSC. Thereover, the primary objective of this study was to identify potential areas for further investigation, thereby establishing a theoretical framework for future therapeutic development.

The primary objective of this study was to investigate the influence of TME-related genes on the development of oncogenesis and OS in patients with LUSC. This study is the first attempt to establish a correlation between clinical parameters and immune and stromal scores in LUSC patients. Our results revealed a statistically significant relationship between immune and stromal scores and various clinicopathological factors, including age, gender, and tumor stage. Additionally, our findings suggest that immune and stromal scores could accurately

Table 3
The correlation between any two of TME-related hub genes.

Correlated gene	Pearson's Correlation	*P*-Value	Cytoband
C3AR1 vs CSF1R	0.88	8.80e-155	5q32
C3AR1 vs CCL2	0.37	3.38e-17	17q12
C3AR1 vs CCR1	0.89	6.16e-164	3p21.31
C3AR1 vs CD14	0.88	1.98e-156	5q31.3
CSF1R vs CCL2	0.42	1.32e-22	17q12
CSF1R vs CCR1	0.82	5.38e-120	3p21.31
CSF1R vs CD14	0.85	1.01e-138	5q31.3
CCL2 vs CCR1	0.40	1.29e-19	3p21.31
CCL2 vs CD14	0.37	5.84e-17	5q31.3
CCR1 vs CD14	0.84	1.35e-130	5q31.3

Table 4
The relationship between TME-related gene mutations and immune cell infiltration.

	B cell	T cell $CD8^+$	T cell $CD4^+$	Macrophage	Neutrophil	DC
C3AR1	0.085	0.36	0.33	**0.044**	0.43	0.24
CSF1R	0.066	0.55	**0.037**	**0.0014**	0.77	0.63
CCL2	NA	NA	NA	NA	NA	NA
CCR1	0.48	0.98	0.41	0.72	0.15	0.12
CD14	0.42	0.7	0.35	0.34	0.35	0.78

predict prognosis in patients with LUSC.

Following stratification into low and high stromal/immune score groups, 946 DEGs were identified. Functional enrichment analyses indicated that these DEGs were primarily associated with the immune response, immune cell differentiation and activation, extracellular matrix, and membrane functions. Furthermore, these molecular functions were significantly associated with surface receptor activity and protein binding. Our study revealed that DEGs were predominantly enriched in immune-related pathways, corroborating previous studies on the influence of TME on tumor growth and invasion, as well as the interplay between immune cells and cancer cells in LUSC [35,36].

A total of 154 significant target genes were identified, with the log-rank test indictating their potential as prognostic markers for OS in LUSC patients. PPI networks were constructed using the STRING tool to establish relationships between the significant target genes. After analyzing of the top six genes (C3AR1, CSF1R, CCL2, CCR1, TYROBP, and CD14), they were identified as hub genes related to the TME. The log-rank test results revealed that five of these hub genes (C3AR1, CSF1R, CCL2, CCR1, and CD14) were associated with poor OS in LUSC patients.

The transcriptional levels of these hub genes in cancer and normal tissues were analyzed using the ONCOMINE database. The ONCOMINE database was used to compare the transcriptional levels of C3AR1, CCL2, CCR1, and CD14 in normal and cancerous lung tissues. Bhattacharjee et al. demonstrated that C3AR1 was under-expressed in LUSC, exhibiting a fold change of −2.759 [37]. Additionally, CCL2 was under-expressed in two lung cancer types: LUSC, (−3.718), and LUAD (−17.989). Selamat discovered that CCL2 was also under-expressed in LUAD, with a fold change of −3.579 [38]. Furthermore, Wachi's study revealed that CCL2 exhibited decreased expression levels in LUSC, with a fold change of −3.417 [39], while Hou et al. demonstrated that CCL2 had fold changes of −3.888 in LUAD patients, −8.396 in large cell lung carcinoma(LCLC), and −4.568 in LUSC patients [40]. In Bhattacharjee's database, CCR1 mRNA expression was low in lung carcinoid cancer, LUSC, and LUAD, while Hou's database showed a decrease in CCR1 expression in LCLC, with a fold change of −4.109 [37]. A consistent pattern was observed in Garber's dataset regarding the differential expression of CD14 in LUSC (fold change = −2.612) and LUAD (fold change = −2.104) (Garber et al., 2001). Garber reported that CD14 was overexpressed in LUAD, with a fold change of 3.769 [41]. Conversely,

Table 5
Significant changes of TME-related hub genes expression in transcription level between lung cancer and normal tissues (ONCOMINE database).

	Types of lung cancer and normal	Fold change	*P* value	*t*-test	Reference
C3AR1	Squamous Cell Lung Carcinoma vs. Normal	−2.759	0.007	−2.577	Bhattacharjee Lung [37]
CSF1R	NA	NA	NA	NA	NA
CCL2	Squamous Cell Lung Carcinoma vs. Normal	−3.718	9.92E-4	−3.455	Bhattacharjee Lung [37]
	Lung Carcinoid Tumor vs. Normal	−17.989	5.12E-7	−6.759	Bhattacharjee Lung [37]
	Lung Adenocarcinoma vs. Normal	−3.579	3.67E-18	−10.249	Selamat Lung [38]
	Squamous Cell Lung Carcinoma vs. Normal	−3.417	0.002	−4.356	Wachi Lung [39]
	Lung Adenocarcinoma vs. Normal	−3.888	2.91E-11	−7.378	Hou Lung [40]
	Large Cell Lung Carcinoma vs. Normal	−8.396	6.36E-8	−7.232	Hou Lung [40]
	Squamous Cell Lung Carcinoma vs. Normal	−4.568	3.12E-10	−7.496	Hou Lung [40]
CCR1	Lung Carcinoid Tumor vs. Normal	−293.774	1.28E-13	−15.558	Bhattacharjee Lung [37]
	Squamous Cell Lung Carcinoma vs. Normal	−14.867	6.37E-6	−5.061	Bhattacharjee Lung [37]
	Lung Adenocarcinoma vs. Normal	−7.001	1.12E-5	−5.356	Bhattacharjee Lung [37]
	Large Cell Lung Carcinoma vs. Normal	−4.109	3.74E-7	−6.792	Hou Lung [40]
	Squamous Cell Lung Carcinoma vs. Normal	−2.612	2.62E-4	−4.531	Garber Lung [41]
	Lung Adenocarcinoma vs. Normal	−2.104	0.001	−3.909	Garber Lung [41]
CD14	Lung Adenocarcinoma vs. Normal	3.769	1.09E-6	6.264	Garber Lung [41]
	Lung Carcinoid Tumor vs. Normal	−16.943	1.38E-8	−7.209	Bhattacharjee Lung [37]
	Small Cell Lung Carcinoma vs. Normal	−6.793	5.54E-5	−4.929	Bhattacharjee Lung [37]
	Lung Adenocarcinoma vs. Normal	−3.821	1.90E-4	−4.241	Bhattacharjee Lung [37]
	Lung Adenocarcinoma vs. Normal	−2.167	3.31E-12	−7.970	Selamat Lung [38]

Bhattacharjee's and Selamat's databases reported that CD14 was under-expressed in lung carcinoid tumors (fold change = −16.943), SCLC (fold change = −6.793), and LUAD (fold change = −3.821 and −2.167, respectively). Notably, CD14 mRNA expression was not detected in LUSC.

One study revealed that the absence of $CD8^+$ T cells in islet tumors was associated with poorer clinical outcomes and decreased lymphocyte function in LUSC patients, whereas CSF1R inhibition improved the migration and infiltration of $CD8^+$ T cells into tumor islets [42]. CSF1R inhibitors may serve as innovative immune-modulating agents for the treatment of tumors [43]. Additionally, a study reported that CCL2 overexpression was associated with progression-free survival and OS in LUSC patients [44]. Wang et al. discovered that suppression of CCR1

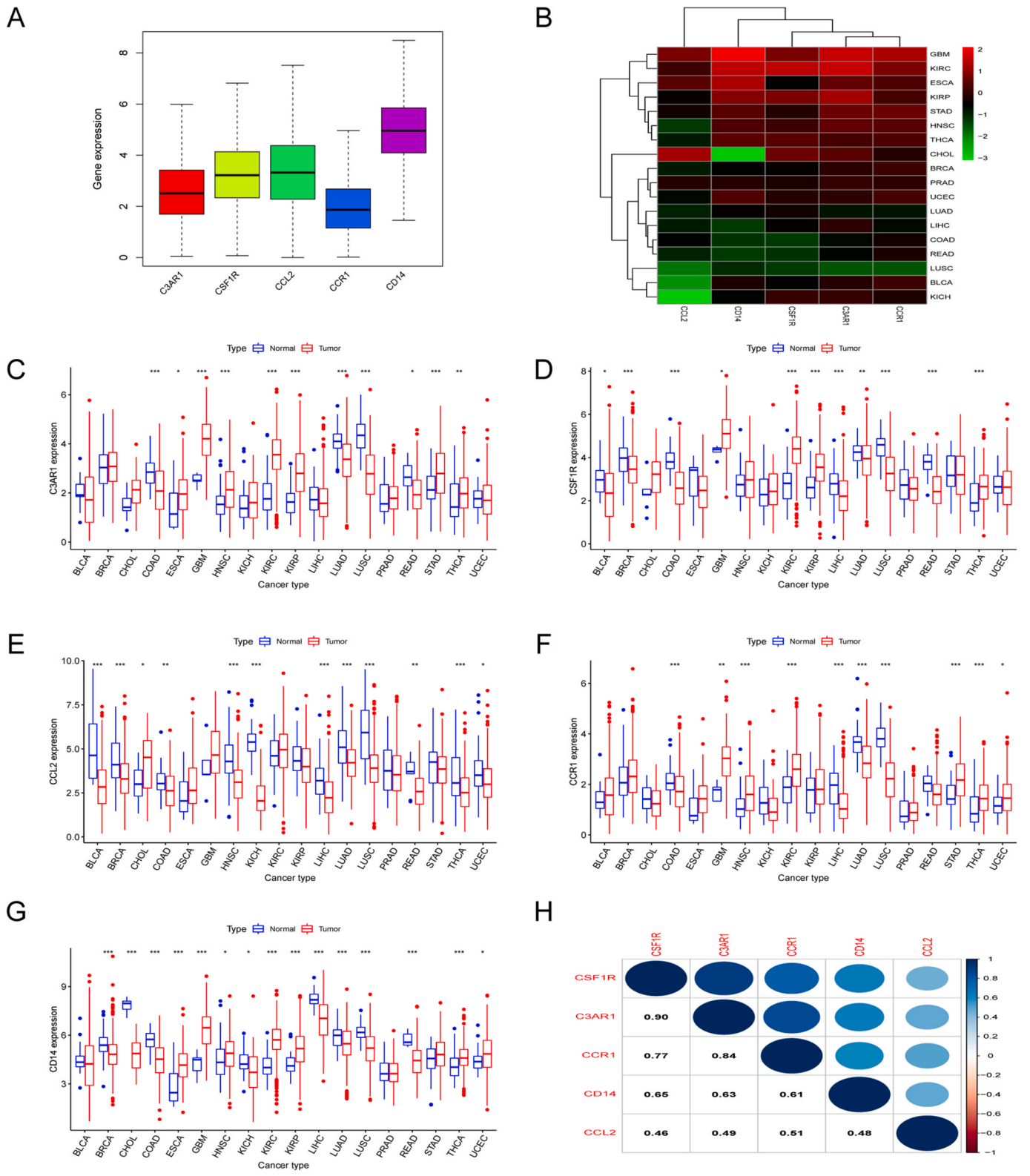

Fig. 8. Expression levels of TME-related prognostic genes in pan-cancers. (**A**) Box plot showing the distribution of TME-related prognostic gene expression across all 33 cancer types. (**B**) Heatmap showing differences in TME-related prognostic gene expression between primary tumors and adjacent normal tissues for 18 cancer types. (**C**) Correlation plot of C3AR1 expression in 18 cancer types. (**D**) Correlation plot of CSF1R expression in 18 cancer types. (**E**) Correlation plot of CCL2 expression in 18 cancer types. (**F**) Correlation plot of CCR1 expression in 18 cancer types. (**G**) Correlation plot of CD14 expression in 18 cancer types. (**H**) Correlation plot based on Spearman correlation test results showing the correlation of gene expression among TME-related genes across all 33 cancer types.

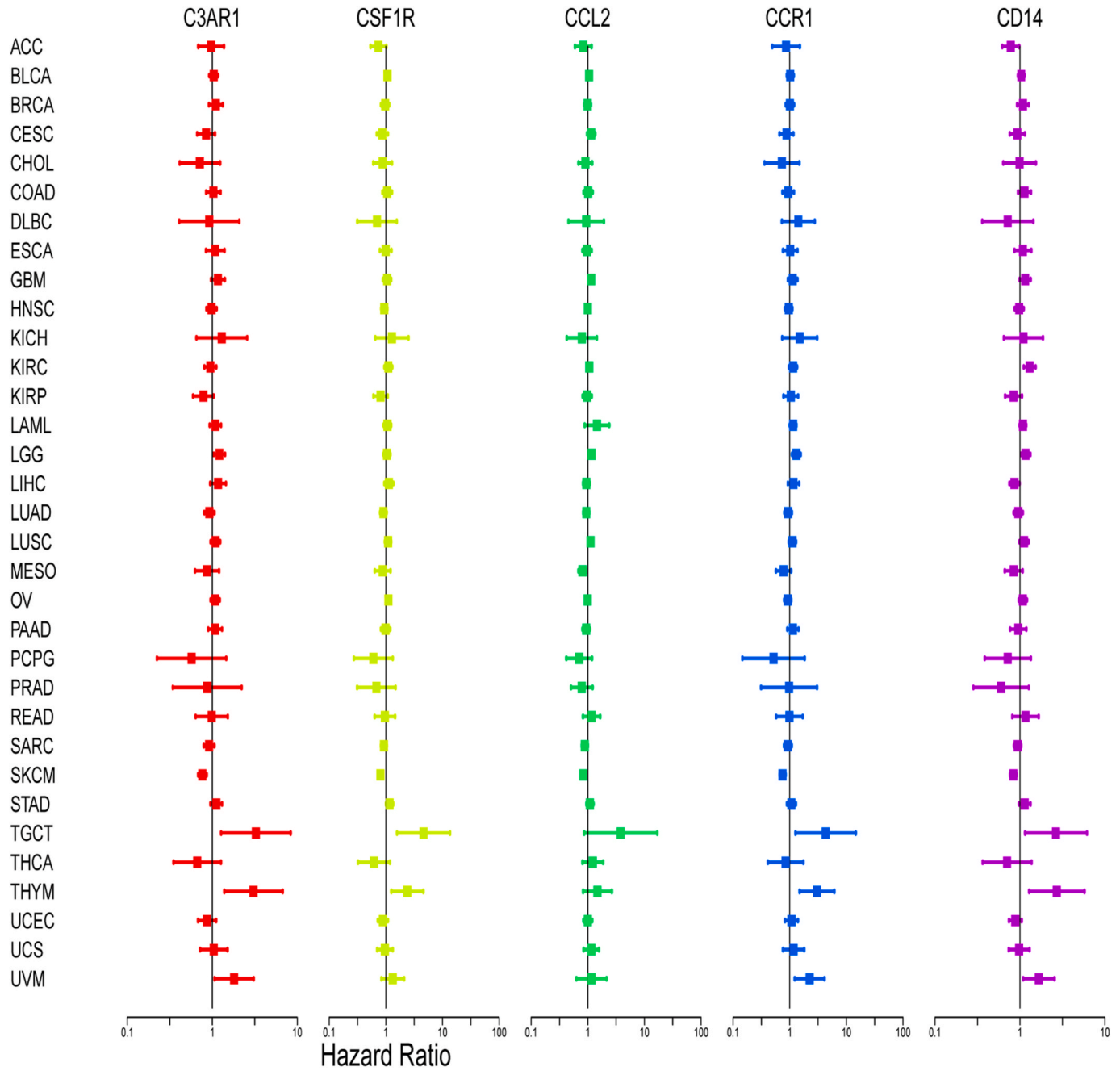

Fig. 9. Relationships between TME-related genes and overall survival in patients with different cancer types. Forest plots with hazard ratios and 95 % confidence intervals showing the survival advantages and disadvantages of increased expression of TME-related genes. Univariate Cox proportional hazard regression models were used for correlation tests.

prevents the invasion of NSCLC cells [45]. While the correlation between C3AR1/CD14 and LUSC is poorly studied, their involvement in immune-related disorders and other cancers has been well documented [46,47]. These data indicate that our findings from the TCGA database have substantial predictive significance. Most central genes identified in our study have not been previously investigated in the context of LUSC, suggesting their potential applicability in the prognostic assessment of patients.

Increasing evidence indicates a significant association between immune cell infiltration and patient outcomes [48,49]. Positive correlations between hub gene expression and immune cell infiltration were identified in this study. Consequently, these genes may provide further insights into clinical outcomes and immune cell infiltration in individuals with LUSC. The mutation rate of these hub genes was 15 % (74/487), and they were associated with OS and DFS. These findings indicate a statistically significant correlation between any pair of hub genes. Furthermore, individuals with gene mutations exhibited heightened immune cell infiltration, particularly macrophages (C3AR1, and CSF1R) and $CD4^+$ T cells (CSF1R).

This study demonstrated that the expression of five TME-related genes differed significantly across most tumors. These genes exhibited inconsistent upregulation or downregulation across various tumors. CCR1 and C3AR1 were predominantly upregulated, whereas CCL2 was downregulated. These results indicate that inherent disparities in the expression of TME-related prognostic genes, not only between different tumor types but also within the same tumor type. Therefore, it is imperative to analyze each independent gene separately. Moreover, TME-related prognostic genes were associated with immune subtypes,

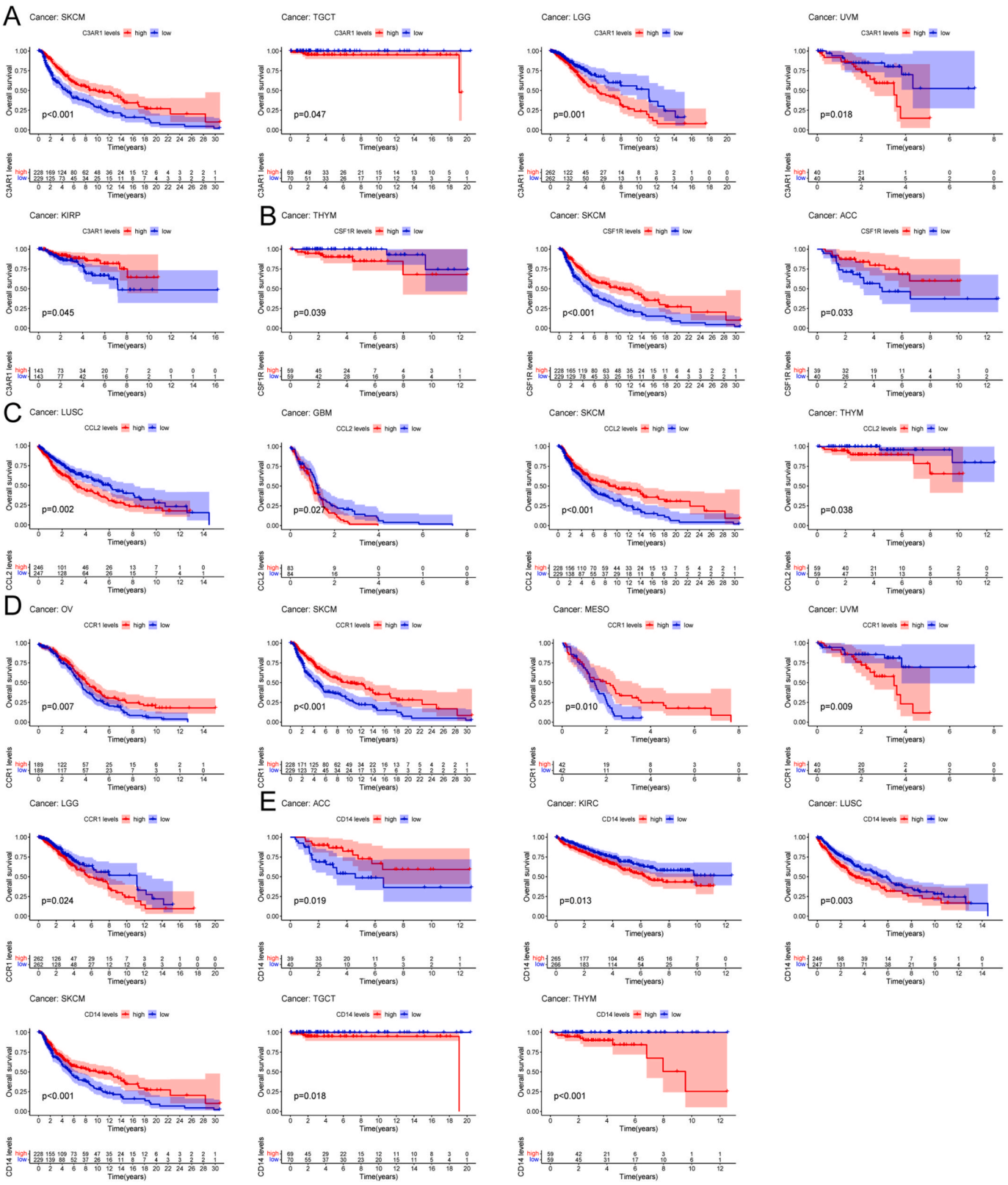

Fig. 10. Survival analysis of patients stratified according to TME-related gene expression across cancers. Overall survival of patients stratified by (**A**) C3AR1, (**B**) CSF1R, (**C**) CCL2, (**D**) CCR1, and (**E**) CD14 expressions across different cancers. The red line indicates high expression, while the blue line indicates low expression.

with varying degrees of correlation observed between different family members and cancer types. In this study, RNAss and DNAss were used to assess the expression of TME-related prognostic genes associated with stem cell-like characteristics [50]. Our findings indicate a negative correlation between TME-related prognostic genes and RNAss, and a positive correlation with DNAss in ACC, OV, THCA, THYM, and UVM. Moreover, a potential correlation was observed between TME-related genes and the sensitivity or resistance of cancer cells to chemotherapy.

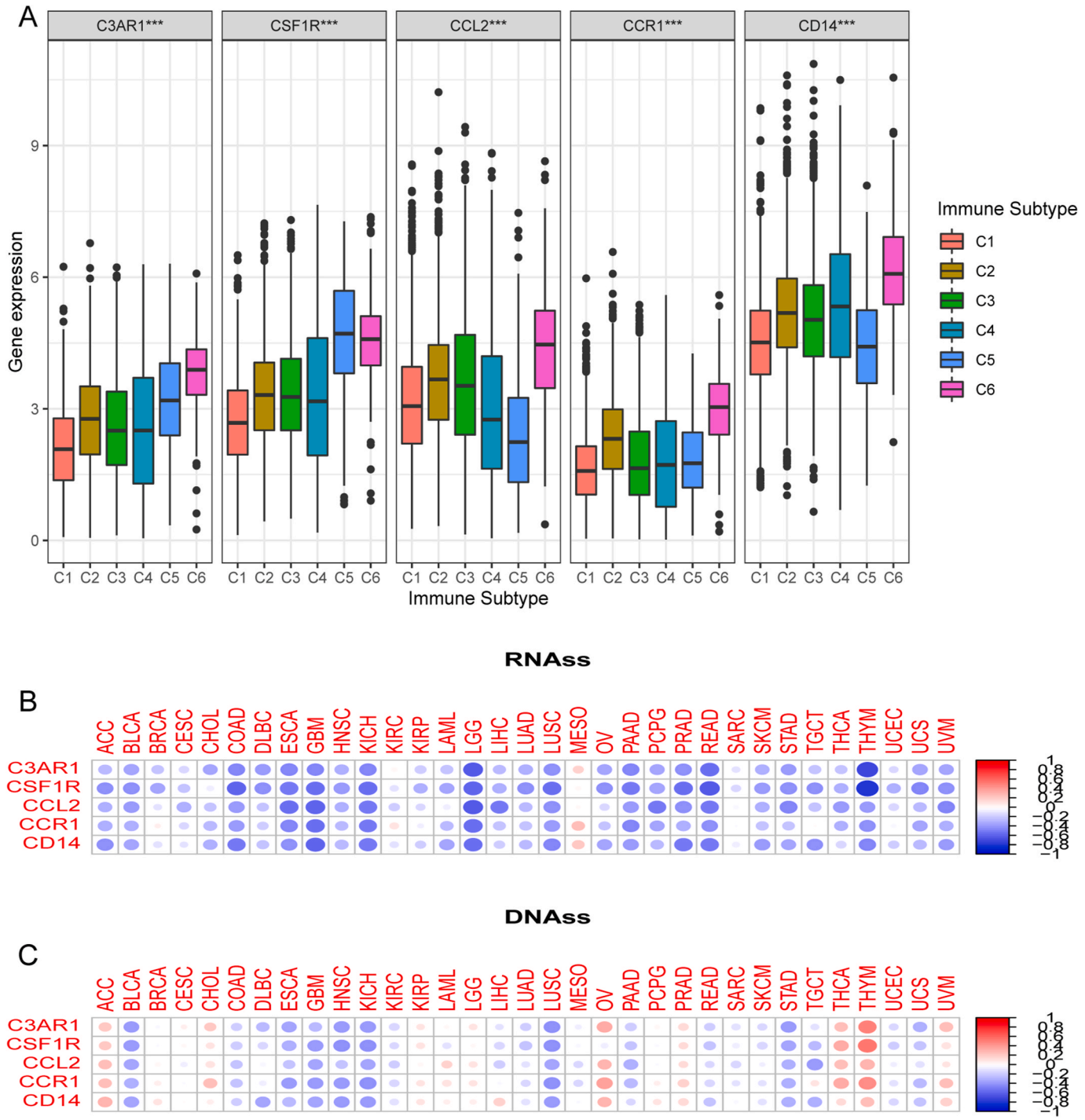

Fig. 11. Association of TME-related gene expression with immune infiltration subtypes and tumor stemness. (**A**) Correlation of TME-related gene expression with immune infiltrate subtypes determined using ANOVA. (**B**) Association between TME-related gene expression and cancer stemness score RNAss based on Spearman's correlation tests. (**C**) Correlation between TME-related gene expression and cancer stemness score DNAss based on Spearman's correlation tests.

The conflicting outcomes suggest that RNAss and DNAss could be used to classify cancer cells into distinct groups based on their unique characteristics or levels of stemness across different types of cancers. Analysis of the data obtained from the NCI-60 cell line revealed that increased expression of TME-related prognostic genes, specifically CCR1 and C3AR1, is associated with resistance to various chemotherapeutic agents. This study offers a comprehensive analysis of the significant influence of TME-related genes on TME, tumor stemness score, and sensitivity to anticancer drugs in humans.

Recently, numerous therapeutic strategies have been developed to target TME-related genes, yielding positive outcomes in clinical trials. In this study, the ESTIMATE algorithm was used to determine the relationship between stromal and immune scores, and the clinicopathological characteristics of patients with LUSC and TME-related prognostic genes with potential as novel biomarkers for LUSC were identified. Despite the significant findings of our study, it is essential to acknowledge its limitations, including its relatively small sample size. Further clinical trials are required to confirm the validity of these findings.

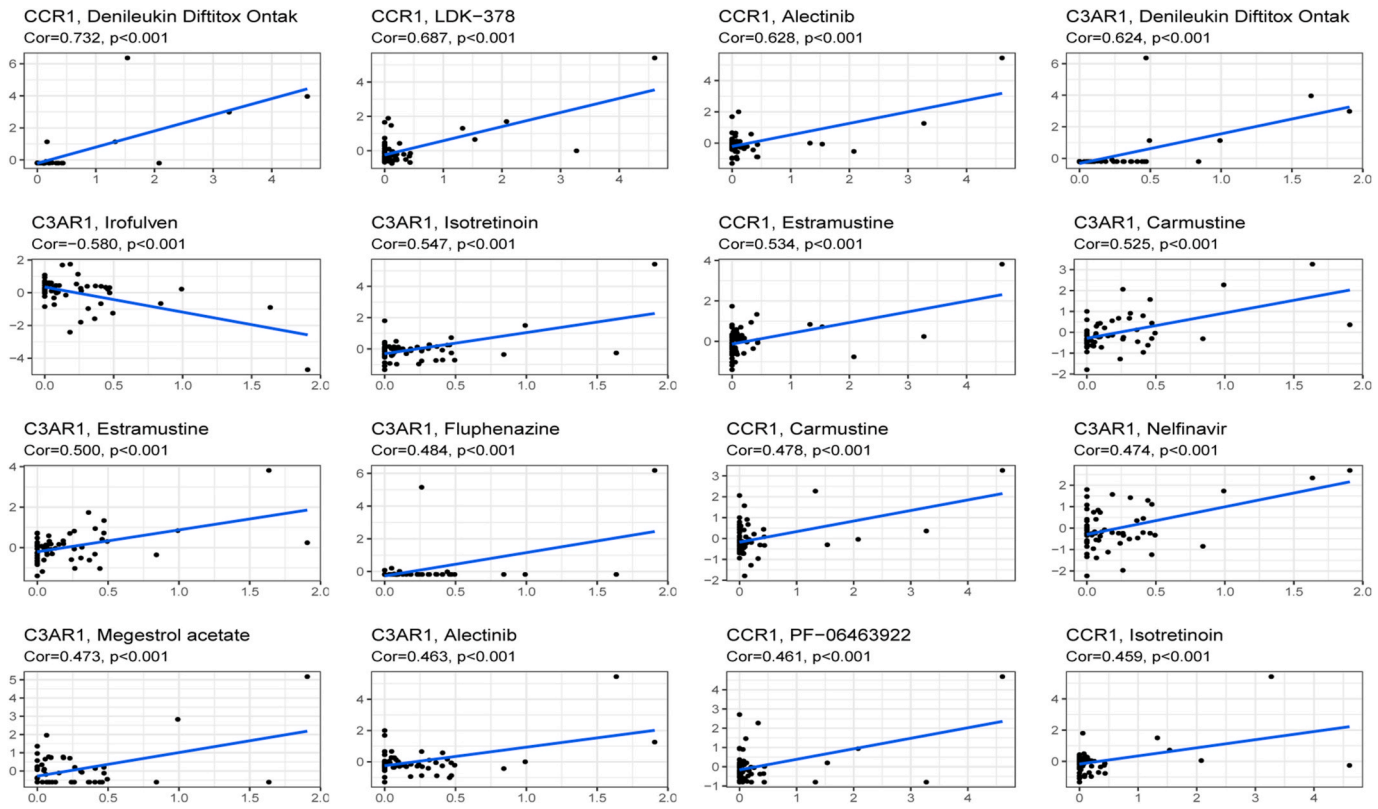

Fig. 12. Association of TME-related gene expression with drug sensitivity.

5. Conclusions

Despite the rapid advancements in targeted therapy and immunotherapy, the overall progression-free survival rate for patients with LUSC remains unsatisfactory. Monitoring biomarkers of the response to targeted treatment is critical for improving the clinical outcomes of patients with LUSC. We analyzed TME-related genes in LUSC using bioinformatic methods and identified five potential prognostic genes: C3AR1, CSF1R, CCL2, CCR1, and CD14. While additional large-scale clinical trials may be necessary to confirm the significance of these genes, they offer promising possibilities for the prognostic assessment of patients diagnosed with LUSC.

Funding statement

This work was supported by the National Natural Science Foundation of China (82173173) and the Traditional Chinese Medicine Science and Technology Project of Shandong Province (2021Q021).

CRediT authorship contribution statement

Xiao Chen: Writing – original draft, Visualization, Funding acquisition, Conceptualization. **Rui Li:** Visualization, Software. **Yun-Hong Yin:** Validation, Conceptualization. **Xiao Liu:** Writing – review & editing, Visualization, Supervision, Software. **Xi-Jia Zhou:** Visualization, Investigation, Conceptualization. **Yi-Qing Qu:** Writing – review & editing, Funding acquisition, Conceptualization.

Declaration of competing interest

The authors declare that there are no conflicts of interest regarding the publication of this paper.

Data availability

Data will be made available on request.

Acknowledgments

This manuscript has been released as a preprint at the Journal of Translational Medicine (https://doi.org/10.21203/rs.3.rs-28076/v1). The preprint introduced the role of TME-related genes in LUSC [51].

References

[1] F. Bray, et al., Global cancer statistics 2018: GLOBOCAN estimates of incidence and mortality worldwide for 36 cancers in 185 countries, CA A Cancer J. Clin. 68 (2018) 394–424, https://doi.org/10.3322/caac.21492.
[2] R.L. Siegel, K.D. Miller, A. Jemal, Cancer statistics, 2020, CA A Cancer J. Clin. 70 (2020) 7–30, https://doi.org/10.3322/caac.21590.
[3] V. Relli, M. Trerotola, E. Guerra, S. Alberti, Abandoning the notion of non-small cell lung cancer, Trends Mol. Med. 25 (2019) 585–594, https://doi.org/10.1016/j.molmed.2019.04.012.
[4] R.S. Herbst, D. Morgensztern, C. Boshoff, The biology and management of non-small cell lung cancer, Nature 553 (2018) 446–454, https://doi.org/10.1038/nature25183.
[5] P. Zhang, et al., Genomic sequencing and editing revealed the GRM8 signaling pathway as potential therapeutic targets of squamous cell lung cancer, Cancer Lett. 442 (2019) 53–67, https://doi.org/10.1016/j.canlet.2018.10.035.
[6] D.S. Shames, I.I. Wistuba, The evolving genomic classification of lung cancer, J. Pathol. 232 (2014) 121–133, https://doi.org/10.1002/path.4275.
[7] C. Gao, et al., Prognostic value of aberrantly expressed methylation gene profiles in lung squamous cell carcinoma: a study based on the Cancer Genome Atlas, J. Cell. Physiol. 234 (2019) 6519–6528, https://doi.org/10.1002/jcp.27389.
[8] Q. Yang, et al., Interaction of ncRNA and epigenetic modifications in gastric cancer: focus on histone modification, Front. Oncol. 11 (2021) 822745, https://doi.org/10.3389/fonc.2021.822745.
[9] L.C. Dieterich, A. Bikfalvi, The tumor organismal environment: role in tumor development and cancer immunotherapy, Semin. Cancer Biol. 65 (2020) 197–206, https://doi.org/10.1016/j.semcancer.2019.12.021.
[10] X. Zhang, et al., Exosomes in cancer: small particle, big player, J. Hematol. Oncol. 8 (2015) 83, https://doi.org/10.1186/s13045-015-0181-x.
[11] J. Galon, et al., The immune score as a new possible approach for the classification of cancer, J. Transl. Med. 10 (2012) 1, https://doi.org/10.1186/1479-5876-10-1.

[12] S. Xiang, et al., Identification of prognostic genes in the tumor microenvironment of hepatocellular carcinoma, Front. Immunol. 12 (2021) 653836, https://doi.org/10.3389/fimmu.2021.653836.
[13] Q. Zhao, et al., Engineered TCR-T cell immunotherapy in anticancer precision medicine: pros and cons, Front. Immunol. 12 (2021) 658753, https://doi.org/10.3389/fimmu.2021.658753.
[14] J. Jin, et al., Identification of genetic mutations in cancer: challenge and opportunity in the new era of targeted therapy, Front. Oncol. 9 (2019) 263, https://doi.org/10.3389/fonc.2019.00263.
[15] K. Yoshihara, et al., Inferring tumour purity and stromal and immune cell admixture from expression data, Nat. Commun. 4 (2013) 2612, https://doi.org/10.1038/ncomms3612.
[16] Y. Guo, et al., Identification of a prognostic ferroptosis-related lncRNA signature in the tumor microenvironment of lung adenocarcinoma, Cell Death Dis. 7 (2021) 190, https://doi.org/10.1038/s41420-021-00576-z.
[17] K. Tomczak, P. Czerwińska, M. Wiznerowicz, The Cancer Genome Atlas (TCGA): an immeasurable source of knowledge, Contemp. Oncol. 19 (2015) A68–A77, https://doi.org/10.5114/wo.2014.47136.
[18] K. Zhao, H. Yang, H. Kang, A. Wu, Identification of key genes in thyroid cancer microenvironment, Med. Sci. Mon. Int. Med. J. Exp. Clin. Res. 25 (2019) 9602–9608, https://doi.org/10.12659/msm.918519.
[19] M.E. Ritchie, et al., Limma powers differential expression analyses for RNA-sequencing and microarray studies, Nucleic Acids Res. 43 (2015) e47, https://doi.org/10.1093/nar/gkv007.
[20] D. Szklarczyk, et al., STRING v11: protein-protein association networks with increased coverage, supporting functional discovery in genome-wide experimental datasets, Nucleic Acids Res. 47 (2019) D607–d613, https://doi.org/10.1093/nar/gky1131.
[21] Z. Tang, et al., GEPIA: a web server for cancer and normal gene expression profiling and interactive analyses, Nucleic Acids Res. 45 (2017) W98–w102, https://doi.org/10.1093/nar/gkx247.
[22] P.J. Thul, C. Lindskog, The human protein atlas: a spatial map of the human proteome, Protein Sci. 27 (2018) 233–244, https://doi.org/10.1002/pro.3307.
[23] T. Li, et al., TIMER: a web server for comprehensive analysis of tumor-infiltrating immune cells, Cancer Res. 77 (2017) e108–e110, https://doi.org/10.1158/0008-5472.Can-17-0307.
[24] J. Gao, et al., Integrative analysis of complex cancer genomics and clinical profiles using the cBioPortal, Sci. Signal. 6 (2013) pl1, https://doi.org/10.1126/scisignal.2004088.
[25] D.R. Rhodes, et al., ONCOMINE: a cancer microarray database and integrated data-mining platform, Neoplasia 6 (2004) 1–6, https://doi.org/10.1016/s1476-5586(04)80047-2.
[26] A. Luna, et al., CellMiner Cross-Database (CellMinerCDB) version 1.2: exploration of patient-derived cancer cell line pharmacogenomics, Nucleic Acids Res. 49 (2021) D1083–d1093, https://doi.org/10.1093/nar/gkaa968.
[27] V. Thorsson, et al., The immune landscape of cancer, Immunity 48 (2018) 812–830.e814, https://doi.org/10.1016/j.immuni.2018.03.023.
[28] D. Tamborero, et al., A pan-cancer landscape of interactions between solid tumors and infiltrating immune cell populations, Clin. Cancer Res. 24 (2018) 3717–3728, https://doi.org/10.1158/1078-0432.Ccr-17-3509.
[29] X. Zhang, B. Klamer, J. Li, S. Fernandez, L. Li, A pan-cancer study of class-3 semaphorins as therapeutic targets in cancer, BMC Med. Genom. 13 (2020) 45, https://doi.org/10.1186/s12920-020-0682-5.
[30] F. Nasim, B.F. Sabath, G.A. Eapen, Lung cancer, Med. Clin. 103 (2019) 463–473, https://doi.org/10.1016/j.mcna.2018.12.006.
[31] D. Waterhouse, et al., Real-world outcomes of immunotherapy-based regimens in first-line advanced non-small cell lung cancer, Lung Cancer 156 (2021) 41–49, https://doi.org/10.1016/j.lungcan.2021.04.007.
[32] D. Zeng, et al., Tumor microenvironment characterization in gastric cancer identifies prognostic and immunotherapeutically relevant gene signatures, Cancer Immunol. Res. 7 (2019) 737–750, https://doi.org/10.1158/2326-6066.Cir-18-0436.
[33] K.B. Givechian, et al., An immunogenic NSCLC microenvironment is associated with favorable survival in lung adenocarcinoma, Oncotarget 10 (2019) 1840–1849, https://doi.org/10.18632/oncotarget.26748.
[34] N. Li, J. Wang, X. Zhan, Identification of immune-related gene signatures in lung adenocarcinoma and lung squamous cell carcinoma, Front. Immunol. 12 (2021) 752643, https://doi.org/10.3389/fimmu.2021.752643.
[35] A. Desrichard, et al., Tobacco smoking-associated alterations in the immune microenvironment of squamous cell carcinomas, J. Natl. Cancer Inst. 110 (2018) 1386–1392, https://doi.org/10.1093/jnci/djy060.
[36] J.S. Seo, et al., Whole exome and transcriptome analyses integrated with microenvironmental immune signatures of lung squamous cell carcinoma, Cancer Immunol. Res. 6 (2018) 848–859, https://doi.org/10.1158/2326-6066.Cir-17-0453.
[37] A. Bhattacharjee, et al., Classification of human lung carcinomas by mRNA expression profiling reveals distinct adenocarcinoma subclasses, Proc. Natl. Acad. Sci. U. S. A. 98 (2001) 13790–13795, https://doi.org/10.1073/pnas.191502998.
[38] S.A. Selamat, et al., Genome-scale analysis of DNA methylation in lung adenocarcinoma and integration with mRNA expression, Genome Res. 22 (2012) 1197–1211, https://doi.org/10.1101/gr.132662.111.
[39] S. Wachi, K. Yoneda, R. Wu, Interactome-transcriptome analysis reveals the high centrality of genes differentially expressed in lung cancer tissues, Bioinformatics 21 (2005) 4205–4208, https://doi.org/10.1093/bioinformatics/bti688.
[40] J. Hou, et al., Gene expression-based classification of non-small cell lung carcinomas and survival prediction, PLoS One 5 (2010) e10312, https://doi.org/10.1371/journal.pone.0010312.
[41] M.E. Garber, et al., Diversity of gene expression in adenocarcinoma of the lung, Proc. Natl. Acad. Sci. U. S. A. 98 (2001) 13784–13789, https://doi.org/10.1073/pnas.241500798.
[42] E. Peranzoni, et al., Macrophages impede CD8 T cells from reaching tumor cells and limit the efficacy of anti-PD-1 treatment, Proc. Natl. Acad. Sci. U. S. A. 115 (2018) E4041–e4050, https://doi.org/10.1073/pnas.1720948115.
[43] M.A. Cannarile, et al., Colony-stimulating factor 1 receptor (CSF1R) inhibitors in cancer therapy, J Immunother Cancer 5 (2017) 53, https://doi.org/10.1186/s40425-017-0257-y.
[44] L. Li, et al., High levels of CCL2 or CCL4 in the tumor microenvironment predict unfavorable survival in lung adenocarcinoma, Thorac Cancer 9 (2018) 775–784, https://doi.org/10.1111/1759-7714.12643.
[45] C.L. Wang, B.S. Sun, Y. Tang, H.Q. Zhuang, W.Z. Cao, CCR1 knockdown suppresses human non-small cell lung cancer cell invasion, J. Cancer Res. Clin. Oncol. 135 (2009) 695–701, https://doi.org/10.1007/s00432-008-0505-0.
[46] J. Su, J. Cui, H.T. Xue, J.H. Tian, J.H. Zhang, Study on the correlation between CD14 gene polymorphism and susceptibility to laryngeal cancer, Eur. Rev. Med. Pharmacol. Sci. 21 (2017) 4292–4297.
[47] S.Y. Wu, et al., C3aR1 gene overexpressed at initial stage of acute myeloid leukemia-M2 predicting short-term survival, Leuk. Lymphoma 56 (2015) 2200–2202, https://doi.org/10.3109/10428194.2014.986481.
[48] J. Li, et al., Tumor characterization in breast cancer identifies immune-relevant gene signatures associated with prognosis, Front. Genet. 10 (2019) 1119, https://doi.org/10.3389/fgene.2019.01119.
[49] T. Kikuchi, et al., Characterization of tumor-infiltrating immune cells in relation to microbiota in colorectal cancers, Cancer Immunol. Immunother. 69 (2020) 23–32, https://doi.org/10.1007/s00262-019-02433-6.
[50] T.M. Malta, et al., Machine learning identifies stemness features associated with oncogenic dedifferentiation, Cell 173 (2018) 338–354.e315, https://doi.org/10.1016/j.cell.2018.03.034.
[51] Xiao Chen, Rui Li, Yun-Hong Yin, et al., Mine TCGA database for tumor microenvironment-related genes of prognostic value in lung squamous cell carcinoma, PREPRINT (Version 1), https://doi.org/10.21203/rs.3.rs-28076/v1, 2020.